RodZ links MreB to cell wall synthesis to mediate MreB rotation and robust morphogenesis

Randy M. Morgenstein[a], Benjamin P. Bratton[a,b], Jeffrey P. Nguyen[c], Nikolay Ouzounov[a], Joshua W. Shaevitz[b,c], and Zemer Gitai[a,1]

[a]Department of Molecular Biology, Princeton University, Princeton, NJ 08544; [b]Lewis-Sigler Institute for Integrative Genomics, Princeton, NJ 08544; and [c]Department of Physics, Princeton University, Princeton, NJ 08544

Edited by Joe Lutkenhaus, University of Kansas Medical Center, Kansas City, KS, and approved September 1, 2015 (received for review May 15, 2015)

The rod shape of most bacteria requires the actin homolog, MreB. Whereas MreB was initially thought to statically define rod shape, recent studies found that MreB dynamically rotates around the cell circumference dependent on cell wall synthesis. However, the mechanism by which cytoplasmic MreB is linked to extracytoplasmic cell wall synthesis and the function of this linkage for morphogenesis has remained unclear. Here we demonstrate that the transmembrane protein RodZ mediates MreB rotation by directly or indirectly coupling MreB to cell wall synthesis enzymes. Furthermore, we map the RodZ domains that link MreB to cell wall synthesis and identify *mreB* mutants that suppress the shape defect of *ΔrodZ* without restoring rotation, uncoupling rotation from rod-like growth. Surprisingly, MreB rotation is dispensable for rod-like shape determination under standard laboratory conditions but is required for the robustness of rod shape and growth under conditions of cell wall stress.

bacterial cytoskeleton | bacterial cell shape | cell growth | cytoskeleton dynamics | robust rod shape

Bacterial cell shape is structurally determined by a rigid peptidoglycan (PG) cell wall built outside of the cytoplasmic membrane by a series of cell wall assembly enzymes (1). In many rod-shaped species these enzymes are coordinated by the actin-like protein, MreB, though the mechanism coupling this cytoplasmic protein to the extracellular cell wall enzymes and the specific functions executed by MreB have remained largely mysterious. Polymeric MreB is necessary to maintain rod-shaped cells, as inhibition of MreB polymerization or deletion of *mreB* cause cells to lose their rod shape. Initially, MreB was thought to form long helical structures that statically define rod shape (2, 3). Later, improved fluorescent fusion proteins and imaging methods revealed that MreB forms short polymers that dynamically rotate around the cell circumference (4–7).

This circumferential rotation requires cell wall synthesis and is conserved across both Gram-negative and Gram-positive species (5–7), leading multiple groups to conclude that rotation promotes rod-shape formation. However, experimentally testing this hypothesis has proven difficult because all previous attempts to disrupt rotation have either led to cell death or massive cell shape changes, making it impossible to isolate the specific function of MreB rotation (5, 6). Furthermore, it remained difficult to explain the mechanistic link between cell wall growth and MreB rotation because of their separation in space by the cytoplasmic membrane. Here, we address both the coupling of MreB to cell wall synthesis and the function of MreB rotation.

Results and Discussion

RodZ Rotates Similarly to MreB. We initially set out to identify proteins necessary for MreB rotation. In *Escherichia coli*, multiple proteins have been suggested to interact with MreB, including the penicillin binding protein (PBP) cell wall synthesis enzymes and RodZ, an integral membrane protein that directly binds MreB (8–11). PBP2 inhibitors block MreB rotation (5) but the PBP2 protein does not have similar dynamics to MreB (12), thus ruling out PBP2 as the major linker between MreB rotation and cell wall synthesis. In contrast, we discovered that RodZ displays similar dynamics to MreB. To covisualize MreB and RodZ dynamics, we expressed a functional GFP–RodZ fusion (*SI Appendix*, Fig. S1) in a strain expressing MreB–msfCFP^{sw} (internal sandwich fusion) from the native *mreB* locus and used time-lapse imaging to track both proteins. RodZ and MreB colocalized in static images (4, 13, 14) and rotated together around the cell circumference in a similar processive fashion, maintaining their colocalization over time (Fig. 1*A*). To establish the statistical significance of MreB–RodZ colocalization, we calculated the Pearson's correlation of MreB and RodZ localization over space and time and compared the resulting correlation with spatially shuffled data. MreB and RodZ fluorescence were correlated over time and their correlation was significant compared with the results of a spatially shuffled model (*SI Appendix*), indicating MreB and RodZ move together during growth (Fig. 1*B*). To our knowledge, RodZ represents the first example of a rod-shape determining protein displaying MreB-like dynamics in *E. coli*.

Three-Dimensional Particle Tracking Establishes That RodZ Is Necessary for MreB Rotation. Given that RodZ is essential for maintaining proper cell shape in *E. coli* (Fig. 2 *A* and *B*), interacts with MreB while spanning the inner membrane (8), and displays similar motion to MreB (Fig. 1), we tested whether RodZ is necessary for MreB rotation by measuring MreB dynamics in a *ΔrodZ* background. To better understand how MreB moves along the 3D

Significance

The bacterial actin homolog, MreB, is a key determinant of rod-cell shape but the mechanism by which it functions has remained a topic of much debate. Recently it was shown that MreB exists as small polymers that actively rotate around the cell circumference. This rotation is widely conserved, yet its mechanism and function have remained unknown. Here we show that MreB rotates because cytoplasmic MreB filaments are coupled to periplasmic cell wall synthesis through the transmembrane protein RodZ, which acts as a transmembrane linker. Furthermore, by genetically uncoupling MreB rotation from growth we establish MreB rotation acts as a robustness mechanism for rod-like shape determination. This work thus explains the mystery of MreB rotation and suggests a new model for bacterial cell shape maintenance.

Author contributions: R.M.M., J.W.S., and Z.G. designed research; R.M.M. and N.O. performed research; R.M.M., B.P.B., J.P.N., and J.W.S. contributed new reagents/analytic tools; R.M.M., B.P.B., J.W.S., and Z.G. analyzed data; and R.M.M. and Z.G. wrote the paper.

The authors declare no conflict of interest.

This article is a PNAS Direct Submission.

Freely available online through the PNAS open access option.

[1]To whom correspondence should be addressed. Email: zgitai@princeton.edu.

This article contains supporting information online at www.pnas.org/lookup/suppl/doi:10.1073/pnas.1509610112/-/DCSupplemental.

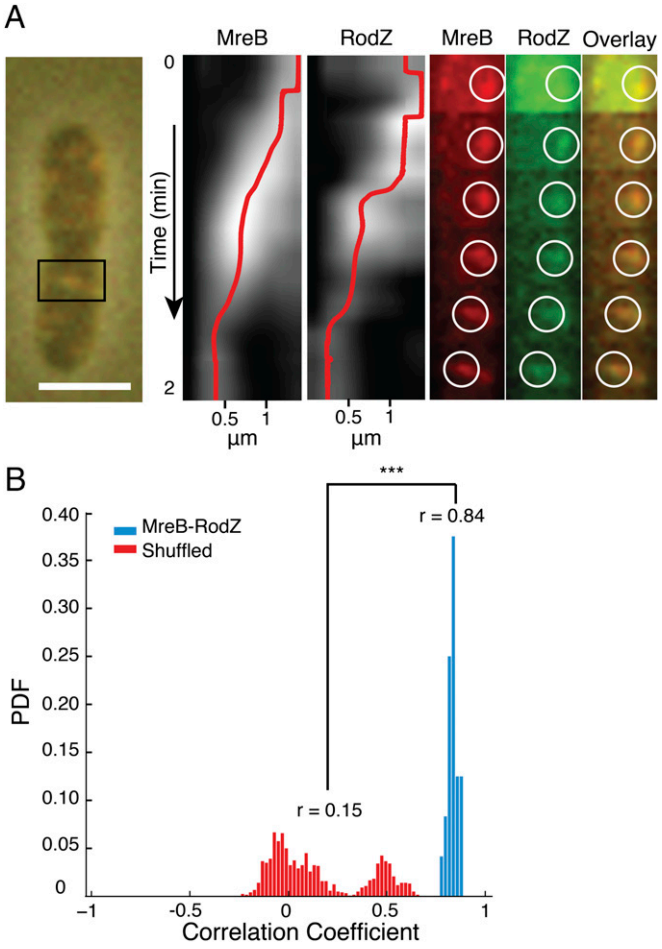

Fig. 1. RodZ motion is correlated with MreB motion. (*A*) Kymograph and time series of MreB–CFP^{sw} and GFP–RodZ. (*Left*) Overlay of phase and fluorescent images. Box indicates section analyzed to make kymographs and time series. (*Middle*) Kymographs with red lines indicating the path of peak intensity of MreB and RodZ foci. (*Right*) Time series depicting movement of the boxed foci (in circles) for both MreB and RodZ. (Scale bar, 2 μm.) (*B*) Pearson's correlation coefficient between MreB and RodZ (blue) and MreB and spatially scrambled RodZ images (red). ***$P < 0.001$.

surface of a cell, we developed a method to track individual MreB–GFP^{sw} foci in 3D (*SI Appendix*, Fig. S2*A*). Each MreB focus was treated as a single point that was tracked by its center of mass. Previously, MreB was tracked solely in its XY position (2D) (5–7), either limiting its detection to a narrow portion of the cell where motion along Z is ignored (5) or requiring use of a statistical correction to account for the missing data in Z (15). Our 3D technique improves upon these efforts by including the data in Z, allowing us to track MreB in abnormally shaped cells, and quantify ∼100-fold more particles than are normally analyzed in 2D studies (*SI Appendix*, Table S1).

The 3D tracking established that in WT cells, MreB moves both clockwise and counterclockwise around the cell circumference, whereas in Δ*rodZ* cells, MreB motion is reduced and less processive (Fig. 2 *C* and *D* and *SI Appendix*, Figs. S2 and S3). To quantify how the loss of RodZ impacts MreB motion, we measured the mean squared displacement (MSD) of MreB foci as a function of time (Fig. 2*C* and *SI Appendix*, Fig. S3). The amount of movement seen along the long axis of the cell was similar to instrument noise as can be seen by the magnitude of the MSD plot (*SI Appendix*, Fig. S2*B*). Though the majority of the MreB motion is circumferential (*SI Appendix*, Fig. S2*B*), we nevertheless report the sum of the MSD of both directions.

Particle motion can be described by fitting the MSD plot to a function with two characteristic parameters, an exponent (α) that signifies the level of processivity (how directed the motion appears), and an offset (Γ) that signifies the overall extent of motion. A diffusive particle will move in a random, nondirected manner with an α equal to one. Diffusion can be seen on the MSD plot by a straight line, or a line with a slope of 1 on a log–log plot. As the α increases, motion becomes more processive until the α reaches 2, where motion is fully ballistic. A processive particle will have an up-sloping curve in the MSD plot, or a line with a slope greater than 1 on the log–log plot. A small change in the value of α will result in a particle exploring a larger area of space and thus can have a significant effect on particle motion. α is measured by taking the slope of the MSD from a log–log plot. Meanwhile, Γ is a proxy for particle speed over short distances, so that when $\alpha = 1$ (diffusion), Γ is proportional to a diffusion constant, and when $\alpha = 2$ (ballistic), Γ is the square of the velocity. Thus, it is possible to eliminate a particle's processivity without eliminating its motion. When two conditions have the same α, the condition with the larger Γ needs less time to explore a given area. However, Γ values are only directly comparable if two particles have the same α. Therefore, to directly compare the speed over short distances of particles with different α, we report τ^* as the time it takes a particle to explore a set area (0.5 μm, the typical size of an MreB focus) (16).

MreB motion is processive and rapid in a WT background ($\alpha = 1.22 \pm 0.06$, $\tau^* = 2.0 \pm 0.1$ min). When *rodZ* is deleted, both the processivity and speed over short distances of MreB significantly decrease ($\alpha = 0.87 \pm 0.06$, $\tau^* = 7.0 \pm 0.7$ min) (Fig. 2*C* and *SI Appendix*, Fig. S3*B*). We note that the residual motion is still quicker than that seen in fixed cells ($\alpha = 0.73 \pm 0.14$, $\tau^* = 46 \pm 13$ min). Thus, RodZ is required for the bulk of processive MreB motion. Interestingly, the deletion of *rodZ* caused MreB to move subdiffusively ($\alpha < 1$). This result may indicate that cell wall synthesis inhibits MreB motion and that such inhibition is relieved by RodZ. Alternatively, the subdiffusive measurement could reflect limitations in our ability to collect data at long time lags.

An MreB Mutant Uncouples Rod Shape from Rotation. Is the dependence of MreB rotation on RodZ due to RodZ coupling MreB to cell wall synthesis or a secondary consequence of the cell shape defects of Δ*rodZ*? To disentangle the roles of RodZ in mediating MreB rotation and rod shape, we performed a screen for mutants that suppressed the Δ*rodZ* round cell shape phenotype. Mutations have been previously found to partially suppress the cell shape defect of Δ*rodZ* (17). Of the mutations found, $MreB_{S14A}$ was focused on for subsequent analysis because it most robustly restored rod shape (Fig. 2 *A* and *B*).

To quantify the rod shape of each cell, we measure cell diameter across the length of the cell body to determine each cell's intracellular diameter deviation as a proxy for rod shape. A true rod will not have any intracellular diameter deviation along the long axis of the cell with deviation only near the poles, and thus will have a smaller intracellular diameter deviation than a round cell that deviates all across its body. To compare populations, we measured the average intracellular diameter deviation for many cells from each background. $MreB_{S14A}$ Δ*rodZ* had less deviation than Δ*rodZ* alone, indicating it restores rod shape (Fig. 2*B*). These cells did not fully phenocopy WT cells in so far as they had an increase in width, indicating a separate role for RodZ in cell shape control. As a control, we introduced $MreB_{S14A}$ into a strain containing wild-type *rodZ* and saw no effect on rod shape (Fig. 2*B*). The ability of *mreB* mutants to restore rod shape in the absence of RodZ indicates that RodZ is not strictly necessary for rod-shape determination.

The mechanism by which $MreB_{S14A}$ suppresses the *rodZ* shape defect remains unclear. *E. coli* MreB associates with the membrane

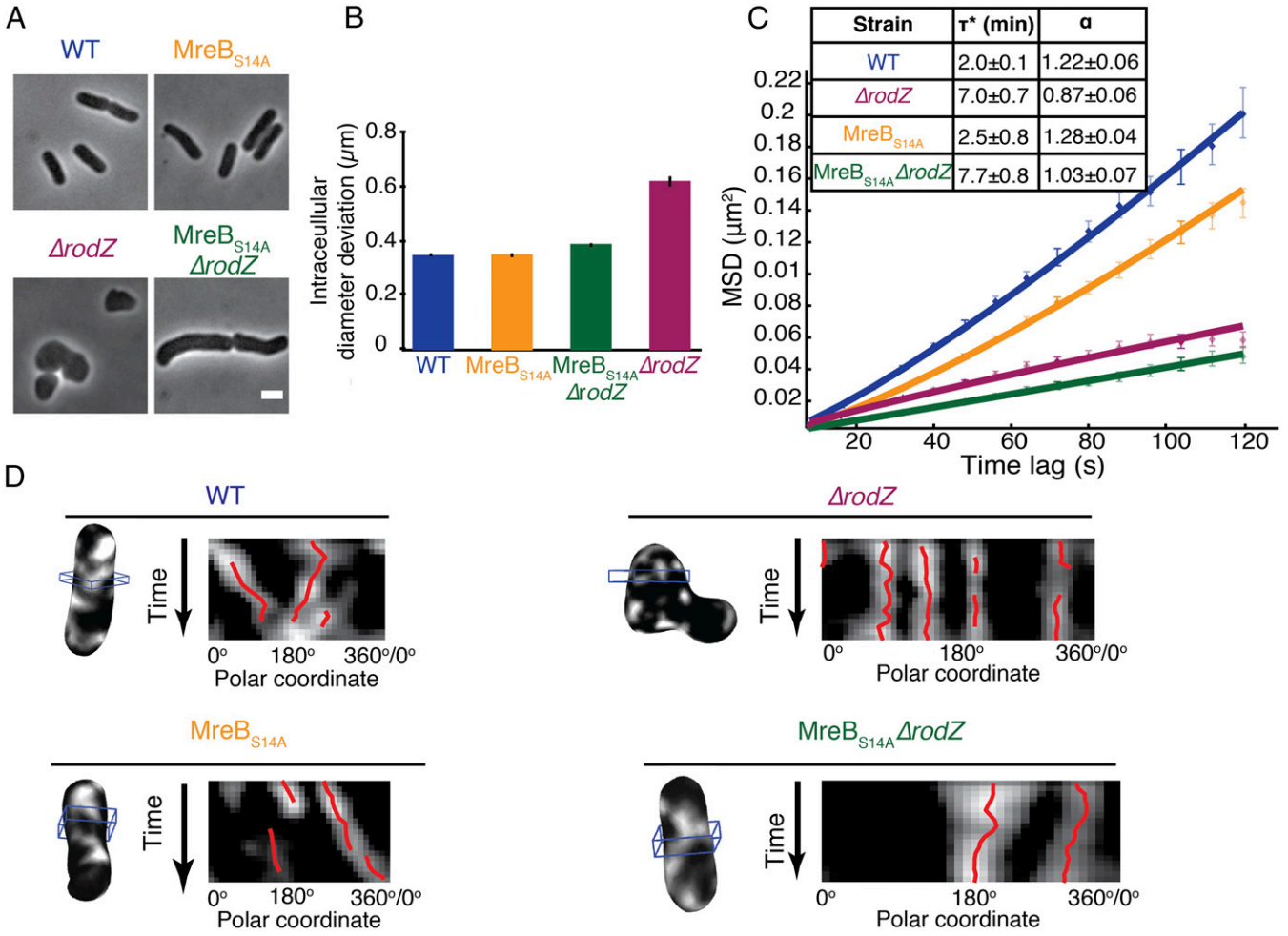

Fig. 2. MreB rotation and rod shape can be uncoupled. (*A*) Phase images showing the cell shape phenotypes of WT, Δ*rodZ*, and MreB suppressor strains. (Scale bar, 2 μm.) (*B*) Diameter deviation is restored to near WT levels in Δ*rodZ* MreB$_{S14A}$. Error bars are bootstrap 95% confidence intervals. (*C*) Mean squared displacement (MSD) of MreB in indicated strain backgrounds. Table displays time for MreB foci to explore 0.2 μm^2 (τ*) and MSD "processivity" exponent (α). (*D*) The 3D reconstructed cells and kymographs of MreB motion. Polar coordinate indicates position of MreB signal on the cell surface orthogonal to the long axis. Because the cell surface wraps back on itself, the left and right ends of the kymograph represent the same point in space.

through its N-terminal amphipathic helix. Residue 14 is in a beta sheet directly after this helix and may promote membrane interaction or protein stability in the absence of RodZ. Development of in vitro assays for MreB assembly and membrane interaction would help determine the exact function of this point mutant.

Importantly, the finding that MreB$_{S14A}$ restored rod-like growth in the absence of RodZ enabled us to finally determine if MreB rotation is necessarily coupled to rod shape. We found that MreB$_{S14A}$ Δ*rodZ* showed little-to-no processive motion of MreB$_{S14A}$ foci (Fig. 2*D*) and quantitatively resembled the motion of MreB$_{WT}$ in spherical *rodZ* deletion mutants (Fig. 2*C*, $\alpha = 1.03 \pm 0.07$, $\tau^* = 7.7 \pm 0.08$ min). To confirm that MreB$_{S14A}$ foci are not intrinsically incapable of motion, we showed that MreB$_{S14A}$ foci moved similarly to MreB$_{WT}$ in the presence of RodZ (Fig. 2*C*, $\alpha = 1.28 \pm 0.04$, $\tau^* = 2.5 \pm 0.8$ min). Thus, RodZ is required for MreB rotation, independent of its role in cell shape determination and MreB rotation is not absolutely required for rod-like morphogenesis.

RodZ Mediates MreB Rotation by Linking Cytoplasmic MreB to Periplasmic PBP2 and/or RodA. How does RodZ mediate MreB rotation? RodZ has both a periplasmic tail that is important for cell shape and could interact with the PBPs and a cytoplasmic tail that directly interacts with MreB (4, 8, 14). To test if RodZ links MreB rotation to cell wall synthesis, truncations in the periplasmic region of RodZ were generated and analyzed for both cell shape and MreB rotation (*SI Appendix*, Fig. S4). Using phase contrast microscopy and a custom metric of cell shape similarity (shape analysis by comparing ensembles of cells represented as Fourier transforms, SPACECRAFT) (*SI Appendix*) we confirmed previous reports that truncating RodZ at amino acid 155 (RodZ$_{1–155}$) has little effect on cell shape (4, 14). As RodZ was truncated further from the periplasmic terminus, cell shape became less rod-like and more similar to Δ*rodZ* (*SI Appendix*, Fig. S4 *B* and *C*). MreB motion became less processive as the periplasmic tail of RodZ was shortened (Fig. 3*A* and *SI Appendix*, Fig. S5 *A* and *C*), with a greater amount of time required to explore 0.2 μm^2 in MSD (Fig. 3*A*). There was only a subtle difference between the MSD of RodZ$_{1–142}$ and full-length RodZ (Fig. 3*A* and *SI Appendix*, Fig. S5*A*) with a change in the processivity of motion, but less of a change in the speed over short distances. However, once the entire periplasmic domain was removed (RodZ$_{1–111}$), MreB motion closely resembled the motion observed in Δ*rodZ* (Fig. 3*A* and *SI Appendix*, Fig. S5*A*). Interestingly, RodZ$_{1–155}$ displayed a slight increase in processivity compared with full-length RodZ (Fig. 3*A*). We hypothesize this slight increase could result from the truncated RodZ protein's

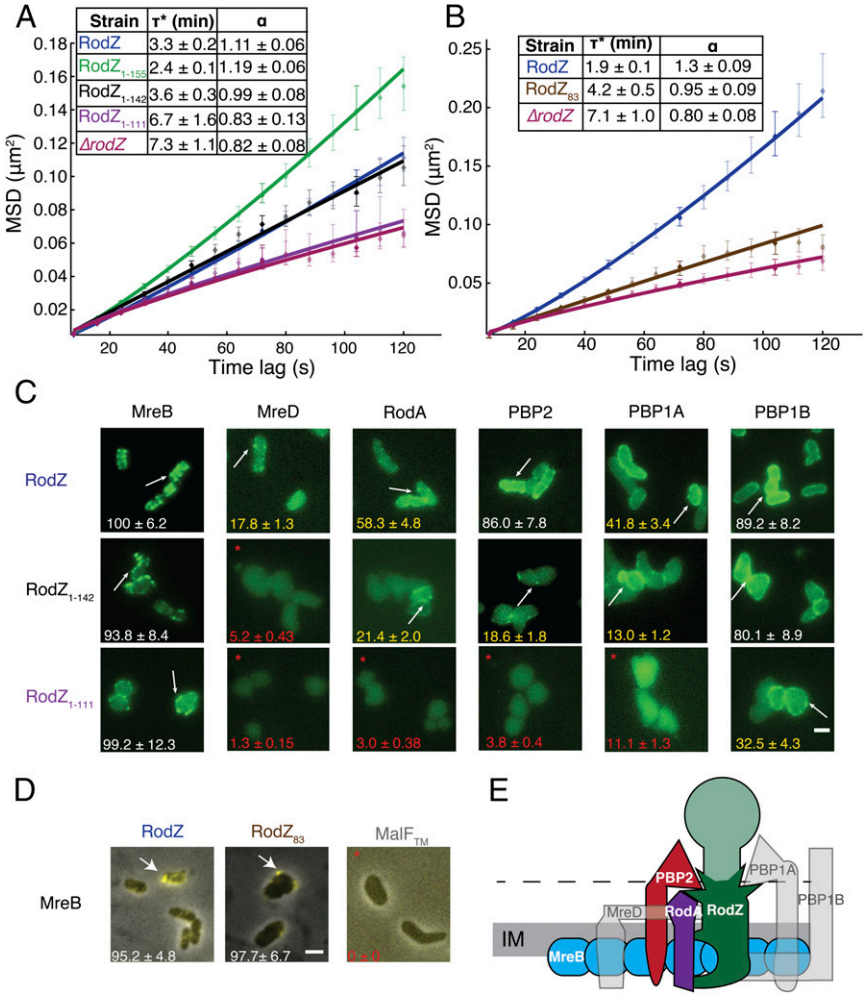

Fig. 3. RodZ acts as a linker to promote MreB rotation through interactions with PBPs. (*A*) MSD of MreB in different RodZ truncation backgrounds. (*B*) MSD of MreB in RodZ cytoplasmic truncation. (*A* and *B*) Tables display time for MreB foci to explore 0.2 μm^2 (τ^*) and MSD exponent (α). (*C*) Bimolecular fluorescence complementation (BiFC) between different RodZ truncations and indicated cell wall synthesis proteins. (*D*) BiFC between MreB and RodZ cytoplasmic truncation. The generic membrane anchor, $MalF_{tm}$ is shown as a negative control. Percent of cells with signal is indicated along with Poisson error to 1 SD. Arrows point to a representative cell displaying signal. White numbers represent over 60% of cells had signal, yellow over 12%, and red and an asterisk less than 12%. The images shown with red numbers display background signal. (Scale bar, 2 μm.) (*E*) Model of RodZ interaction partners. Faded out proteins are not thought to be important for MreB rotation. Proteins represented in different colors are shown interacting at specific regions of RodZ. MreB is shown as a polymer.

smaller size causing less drag or from the truncated region interacting with accessory factors.

Our results suggest that RodZ uses its periplasmic tail to link MreB motion to a protein(s) in the periplasm. To further test this RodZ linker model, we attempted to uncouple MreB from RodZ on the cytoplasmic side of the inner membrane by deleting most of its cytoplasmic domain ($RodZ_{83}$). This cytoplasmic truncation exhibited a round shape similar to that of *ΔrodZ* (*SI Appendix*, Fig. S4 *B* and *C*). As expected for a mutant that reduces the coupling of MreB to cell wall synthesis, we observed a significant reduction in both the processivity and speed over short distances of MreB motion in $RodZ_{83}$ (Fig. 3*B* and *SI Appendix*, Fig. S5 *B* and *D*). To address the possibility that the slight remaining motion was due to the irregular cell shape, we moved $RodZ_{83}$ into the $MreB_{S14A}$ background. $MreB_{S14A}$ suppressed the cell shape defect of $RodZ_{83}$ but the slight MreB motion remained, although it is still significantly less processive and less quick than WT (*SI Appendix*, Fig. S5 *E* and *F*).

We noted that in contrast to deleting the periplasmic domain ($RodZ_{1–111}$), deleting the previously characterized MreB-binding domain (8) ($RodZ_{83}$) did not completely eliminate MreB motion (Fig. 3*B* and *SI Appendix*, Fig. S5). One explanation for the surprising residual MreB motion in $RodZ_{83}$ is that this truncation does not completely eliminate the interaction between RodZ and MreB. To test this possibility, a bimolecular fluorescence complementation assay (BiFC) was developed and validated to characterize RodZ's interaction partners (See *SI Appendix* for assay details and controls and *SI Appendix*, Fig. S6) (18, 19). BiFC works by separating YFP into two nonfluorescent domains. These domains, if brought together, can form a functional fluorescent molecule. To test if proteins interact, each YFP domain is translationally fused to a protein of interest. If these proteins interact, fluorescence is restored, but if the proteins do not interact, then YFP remains nonfunctional. To validate the assay, MreB was tagged at an internal site (4), and RodZ was tagged on both its N and C termini. As expected, MreB–RodZ BiFC signal was only observed when the tag was present on the cytoplasmic N teminus of RodZ (Fig. 3*C* and *SI Appendix*, Fig. S6). To validate the functionality of the BiFC interaction between MreB and RodZ, we examined it in a strain expressing MreB–$mCherry^{SW}$ at the native *mreB* locus (4). We observed that the BiFC signal colocalizes with the native MreB, indicating the BiFC has a proper

cellular localization. Previous studies have suggested that BiFC produces binary results (20). To quantify if a pair of BiFC partners interacted, we thus determined the fraction of cells whose BiFC fluorescence signal was significantly greater than that of negative controls.

As predicted by the residual MreB motion, residual interaction between MreB and RodZ could still be detected even upon deleting the previously characterized helix-turn-helix MreB-binding motif of RodZ (8) ($RodZ_{83}$) (Fig. 3*D*). The only cytoplasmic portion of RodZ remaining in $RodZ_{83}$ is the basic juxtamembrane domain (*SI Appendix*, Fig. S4*A*), which we suggest represents a previously unidentified MreB-binding site. Because $RodZ_{83}$ does lose rod shape, we propose that the helix-turn-helix interaction site may explain the rotation-independent morphogenesis roles of RodZ, whereas the juxta-membrane RodZ–MreB interaction site may enhance MreB rotation and explain the recent report that MreB is intimately membrane associated (21). The two MreB-binding sites may also partially functionally overlap as $RodZ_{83}$ does not fully phenocopy the *ΔrodZ* cell shape phenotype (*SI Appendix*, Fig. S4). It is also possible that this residual motion reflects an interaction between MreB and another protein involved in cell wall synthesis.

Having established the BiFC assay, we also used it to address which cell wall synthesis proteins RodZ interacts with to link MreB rotation to growth. Specifically, we examined the interactions between RodZ and PBP1A, PBP1B, PBP2, RodA, MreB, MreC, and MreD (Fig. 3*C*). RodZ interacted with all of the candidate proteins except for MreC (*SI Appendix*, Fig. S7*A*). In an effort to narrow down the remaining candidates, we tested the RodZ periplasmic truncations to determine which interactions are lost in the truncations that disrupt MreB rotation. Importantly, all of the RodZ truncations maintained the interaction with MreB (Fig. 3*C*). $RodZ_{1–111}$ no longer has the *rodZ* transmembrane domain but continued to interact with both PBP1B and MreB, indicating that RodZ does not need its transmembrane domain to interact with MreB and that PBP1B binding is not sufficient for MreB rotation. Interaction of MreD with RodZ was disrupted by the $RodZ_{1–142}$ truncation in which MreB still rotates (Fig. 3 *A* and *C*), and MreB continued to rotate in a *pbp1A* deletion (*SI Appendix*, Fig. S7*B*), ruling out MreD and PBP1A as the major contributors to MreB rotation. In all cases, the loss of the RodZ interactions with PBP2 and RodA correlated with the loss of MreB rotation. Thus, we conclude that RodZ mediates MreB rotation by coupling MreB to PBP2 and/or RodA activity (Fig. 3*E*).

These results are consistent with previous findings that inhibition of PBP2 but not PBP1A stops MreB motion and that a *pbp2* temperature-sensitive allele reduces MreB motion (5). Because PBP2 is a peptidoglycan transpeptidase and none of the known transglycosylases are required, transpeptidation might be responsible for the bulk of MreB motion. It is also possible that an unknown transglycosylase is involved.

MreB Rotation Functions as Mechanism for Robust Rod-Like Growth. MreB rotation is widely conserved, so if it is not required for rod shape, then what is its function? One possibility is that rotation facilitates the initiation of rod shape. However, spherical L-forms (cells lacking a cell wall) made from $MreB_{S14A}$*ΔrodZ* cells were still able to reestablish rod shape, indicating that MreB rotation is not needed for the initiation of rod shape (*SI Appendix*, Fig. S8*A*). Another possibility is that MreB rotation enhances the robustness of rod shape to facilitate growth in the presence of osmotic or PG stress. When MreB is unable to rotate ($MreB_{S14A}$*ΔrodZ*), cells that grew as rods in LB media (~0.4 Osm) became spheroid under the osmotic stress of growth in LB supplemented with NaCl (~1.1 Osm) or sucrose (~1.0 Osm) (Fig. 4*A* and *SI Appendix*, Fig. S9*A*). Whereas the $MreB_{S14A}$*ΔrodZ* cells did not become perfectly spheroid in osmotic media (as *ΔrodZ*), they still lost rod shape. Confirming that MreB rotation is not required for rod initiation, $MreB_{S14A}$*ΔrodZ* cells grown in high osmotic media quickly recovered to form rods when osmotic pressure was removed, even though rotation is not restored when cells are grown in high osmolality (*SI Appendix*, Fig. S8 *B–E*). Cells with an intermediate rotation phenotype ($MreB_{S14A}RodZ_{83}$) were resistant to the shape changes induced by osmotic stress (*SI Appendix*, Fig. S9 *B* and *C*), indicating that only a little MreB rotation is needed to supply protection against osmotic stress. As another form of PG stress, we examined growth in the presence of mecillinam, which inhibits the PBP2 cell wall transpeptidase enzyme (22). Rod cells were more sensitive to PBP2 inhibition when MreB rotation was inhibited (Fig. 4*B*). In addition to suggesting that rotation promotes robustness to cell wall stress, the sensitivity of these rods to PBP2 inhibition indicates that PBP2 is still active in these cells. This result supports our hypothesis that RodZ functions by linking PBP2/RodA activity to MreB rather than by directly modulating PBP2 activity.

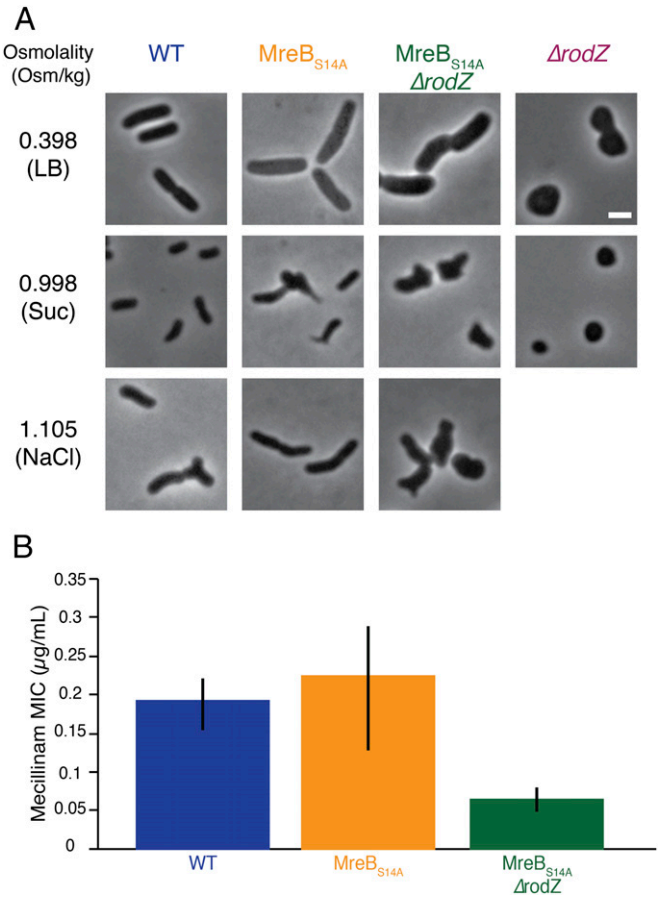

Fig. 4. MreB rotation is needed for growth under cell wall stresses. (*A*) MreB rotation is important for growth in high osmolality. (Scale bar, 2 μm.) (*B*) MreB rotation is important for growth when PBP2 is inhibited by mecillinam treatment. Not shown is *ΔrodZ*, which is mellicinam resistant. Error bars represent SD.

Because MreB rotation depends on cell wall growth but MreB is in a different cellular compartment than the cell wall, there must be a linker protein that connects the two. Here we showed that RodZ couples MreB to cell wall synthesis by interacting with MreB in the cytoplasm and PBP2 and/or RodA in the periplasm. RodZ thus plays two separable roles, mediating both rod-like growth and MreB rotation. Our studies suggest that the rod growth function of RodZ is mediated by its interactions with MreB through its helix-turn-helix motif, whereas a previously

undefined juxta-membrane MreB-binding site promotes RodZ's role in linking cell wall synthesis to MreB rotation.

Our model suggests that RodZ acts as a linker that keeps MreB coupled to cell wall synthesis to generate processive motion. Because MreB can direct rod formation in the absence of RodZ, MreB may maintain its ability to initiate the sites of new cell wall synthesis in a rotation-independent manner, either directly or through a second linker protein.

Conclusions

Because RodZ is highly conserved but its role in rod shape determination can be readily suppressed (Fig. 2 and ref. 17), we suggest that RodZ's additional role in MreB rotation provides an important beneficial function. Specifically, RodZ-mediated MreB rotation enables cells to robustly build the cell wall to withstand external stresses. The importance of rotation in promoting rod growth in a variety of environments and stresses can be explained by computational modeling showing that MreB rotation enables cells to more evenly distribute new PG synthesis throughout the rod (5, 23). The combination of the previous simulations with our previously unidentified data suggest that MreB directs the sites of new cell wall synthesis (24) independently of RodZ. RodZ then couples MreB to the cell wall synthesis apparatus once it has been recruited, such that when MreB is stationary (*ΔrodZ*), new cell wall keeps inserting at the same sites. This organization can still give rise to rod-like shape when the cell wall is well ordered, as when grown in nutrient-rich media, but local defects induced by stress are amplified, leading to dramatic changes in steady-state shape (5). Thus, whereas it had been previously hypothesized that MreB rotation was important for rod shape, direct testing of this hypothesis shows rotation is not essential for rod-like growth but rather acts to help cells adapt to different growth conditions. These findings are consistent with recent studies demonstrating that MreB mediates the initiation and maintenance of rod shape through its localization to areas of negative Gaussian curvature (24, 25). When local defects occur from cell wall stress, MreB rotation prevents these local defects from being amplified. Thus, MreB localization appears to determine the basic rod shape, whereas MreB dynamics promote robust rod-like morphogenesis.

Methods

Bacterial Growth. Bacteria were grown using standard laboratory conditions. Cultures were grown overnight in LB medium, subcultured in the morning 1:1,000, and grown to exponential phase. Plasmids were electroporated into S17 *E. coli* and then subcloned into the appropriate strain using transformation and storage solution buffer. When required cells were induced with isopropyl β-D-1-thiogalactopyranoside or arabinose and grown with the proper antibiotics. For information about *rodZ* expression, BiFC strains, minimal inhibitory concentration (MIC), and osmotic growth see *SI Appendix*, *SI Methods* and Tables S2 and S3.

Microscopy. Cells were grown at 37 °C in LB or indicated media. Imaging was done on M63 glucose plus casamino acid pads with 1% agarose at room temperature. Phase contrast images and 2D time-lapse movies were collected on a Nikon90i epifluorescent microscope equipped with a 100×/1.4 N.A. objective (Nikon), Rolera XR cooled CCD camera (QImaging), and NIS Elements software (Nikon). Images for 3D particle tracking were taken on a monolithic aluminum microscope (homemade) with a 100×/1.49 N.A. (Nikon) objective, iXon DU897 cooled EMCCD camera (Andor Technology), and a homemade LabView software package (National Instruments) (see *SI Appendix* for details).

Cell-Shape Analysis. For 2D analysis phase images were analyzed using the MATLAB script Morphometrics to obtain cell contours. These contours were analyzed by our custom metric for cell shape SPACECRAFT. This was used to compare similarity between the distributions of shapes observed in different RodZ truncation strains. The 3D cell contours were obtained by minimizing the difference between an observed Z stack and the forward convolution of a model with the experimental point spread function (24). We improved upon this method by introducing triangular meshing to more accurately determine both rod- and nonrod-shaped cells (see *SI Appendix* for details).

Three-Dimensional Tracking. Because MreB is membrane bound, we tracked MreB's motion in the plane of the surface. Each MreB focus was treated as a single point, whose center of mass was tracked. For each focus, we calculated the MSD between all time points separated by time lag τ. These individual track MSDs were averaged together and fit to a two-parameter model: $\mathrm{MSD}(\tau) = \Gamma\tau^{\alpha}$. Γ informs about the speed over short distances but carries units of $\mu m^2/sec^{\alpha}$, and α represents processivity. Confidence regions on both parameters were estimated from a bootstrap analysis (see *SI Appendix* for more details).

ACKNOWLEDGMENTS. We thank Tom Silhavy, Phil Rather, and Elizabeth Ohneck for careful reading of this manuscript and the members of the Z.G. and J.W.S. laboratories for technical assistance and advice. R.M.M. and Z.G. are funded by National Institute of General Medical Sciences Grants F32 GM103290-01A1 and 1RO1GM107384. B.P.B. was funded by National Science Foundation Career Grant PHY-0844466 (to J.W.S.) and NIH Grant P50 GM071508.

1. Typas A, Banzhaf M, Gross CA, Vollmer W (2012) From the regulation of peptidoglycan synthesis to bacterial growth and morphology. *Nat Rev Microbiol* 10(2):123–136.
2. Swulius MT, Jensen GJ (2012) The helical MreB cytoskeleton in *Escherichia coli* MC1000/pLE7 is an artifact of the N-terminal yellow fluorescent protein tag. *J Bacteriol* 194(23):6382–6386.
3. Jones LJF, Carballido-López R, Errington J (2001) Control of cell shape in bacteria: Helical, actin-like filaments in Bacillus subtilis. *Cell* 104(6):913–922.
4. Bendezú FO, Hale CA, Bernhardt TG, de Boer PAJ (2009) RodZ (YfgA) is required for proper assembly of the MreB actin cytoskeleton and cell shape in *E. coli*. *EMBO J* 28(3):193–204.
5. van Teeffelen S, et al. (2011) The bacterial actin MreB rotates, and rotation depends on cell-wall assembly. *Proc Natl Acad Sci USA* 108(38):15822–15827.
6. Domínguez-Escobar J, et al. (2011) Processive movement of MreB-associated cell wall biosynthetic complexes in bacteria. *Science* 333(6039):225–228.
7. Garner EC, et al. (2011) Coupled, circumferential motions of the cell wall synthesis machinery and MreB filaments in *B. subtilis*. *Science* 333(6039):222–225.
8. van den Ent F, Johnson CM, Persons L, de Boer P, Löwe J (2010) Bacterial actin MreB assembles in complex with cell shape protein RodZ. *EMBO J* 29(6):1081–1090.
9. Kruse T, Bork-Jensen J, Gerdes K (2005) The morphogenetic MreBCD proteins of *Escherichia coli* form an essential membrane-bound complex. *Mol Microbiol* 55(1):78–89.
10. Figge RM, Divakaruni AV, Gober JW (2004) MreB, the cell shape-determining bacterial actin homologue, co-ordinates cell wall morphogenesis in *Caulobacter crescentus*. *Mol Microbiol* 51(5):1321–1332.
11. Varma A, Young KD (2009) In *Escherichia coli*, MreB and FtsZ direct the synthesis of lateral cell wall via independent pathways that require PBP 2. *J Bacteriol* 191(11):3526–3533.
12. Lee TK, et al. (2014) A dynamically assembled cell wall synthesis machinery buffers cell growth. *Proc Natl Acad Sci USA* 111(12):4554–4559.
13. Alyahya SA, et al. (2009) RodZ, a component of the bacterial core morphogenic apparatus. *Proc Natl Acad Sci USA* 106(4):1239–1244.
14. Shiomi D, Sakai M, Niki H (2008) Determination of bacterial rod shape by a novel cytoskeletal membrane protein. *EMBO J* 27(23):3081–3091.
15. Liu Z, et al. (2014) Super-resolution imaging and tracking of protein-protein interactions in sub-diffraction cellular space. *Nat Commun* 5:4443.
16. Ouzounov N, et al. (2015) . MreB helical pitch angle determines cell diameter in *Escherchia coli*. arXiv:1503.07789.
17. Shiomi D, et al. (2013) Mutations in cell elongation genes *mreB, mrdA* and *mrdB* suppress the shape defect of RodZ-deficient cells. *Mol Microbiol* 87(5):1029–1044.
18. Kerppola TK (2008) Bimolecular fluorescence complementation (BiFC) analysis as a probe of protein interactions in living cells. *Annu Rev Biophys* 37(1):465–487.
19. Magliery TJ, et al. (2005) Detecting protein-protein interactions with a green fluorescent protein fragment reassembly trap: Scope and mechanism. *J Am Chem Soc* 127(1):146–157.
20. Kerppola TK (2009) Visualization of molecular interactions using bimolecular fluorescence complementation analysis: Characteristics of protein fragment complementation. *Chem Soc Rev* 38(10):2876–2886.
21. van den Ent F, Izoré T, Bharat TA, Johnson CM, Löwe J (2014) Bacterial actin MreB forms antiparallel double filaments. *eLife* 3(e02634):e02634.
22. Spratt BG (1977) The mechanism of action of mecillinam. *J Antimicrob Chemother* 3(Suppl B):13–19.
23. Furchtgott L, Wingreen NS, Huang KC (2011) Mechanisms for maintaining cell shape in rod-shaped Gram-negative bacteria. *Mol Microbiol* 81(2):340–353.
24. Ursell TS, et al. (2014) Rod-like bacterial shape is maintained by feedback between cell curvature and cytoskeletal localization. *Proc Natl Acad Sci USA* 111(11):E1025–E1034.
25. Billings G, et al. (2014) De novo morphogenesis in L-forms via geometric control of cell growth. *Mol Microbiol* 93(5):883–896.